

Looking for the Best Constant in a Sobolev Inequality: A Numerical Approach

Alexandre Caboussat^{1,*}, Roland Glowinski^{2,3}, Allison Leonard⁴

¹ Department of Mathematics, University of Houston, 4800 Calhoun Rd, Houston, Texas 77204 - 3008, USA. e-mail: caboussat@math.uh.edu

² Department of Mathematics, University of Houston, 4800 Calhoun Rd, Houston, Texas 77204 - 3008, USA. e-mail: roland@math.uh.edu

³ Institute of Advanced Studies, The Hong Kong University of Science and Technology, Clear Water Bay, Kowloon, Hong Kong

⁴ Department of Mathematics, University of Houston, 4800 Calhoun Rd, Houston, Texas 77204 - 3008, USA. e-mail: aleonard@math.uh.edu

Received: date / Revised version: date

Dedicated to Professor Richard Tapia on the occasion of his 70th birthday.

Abstract. A numerical method for the computation of the best constant in a Sobolev inequality involving the spaces $H^2(\Omega)$ and $C^0(\overline{\Omega})$ is presented. Green's functions corresponding to the solution of Poisson problems are used to express the solution. This (kind of) non-smooth eigenvalue problem is then formulated as a constrained optimization problem and solved with two different strategies: an augmented Lagrangian method, together with finite element approximations, and a Green's functions based approach. Numerical experiments show the ability of the methods in computing this best constant for various two-dimensional domains, and the remarkable convergence properties of the augmented Lagrangian based iterative method.

Key words. Sobolev inequality – Augmented Lagrangian algorithm – Finite elements method – Distributed optimal control – Uzawa algorithm.

* Corresponding author

Mathematics Subject Classification (2000): 90C30, 65K10, 47A75, 49M37, 65N30

1. Introduction

Suppose that Ω is a bounded domain of \mathbb{R}^d with $d \in \{1, 2, 3\}$. It is well known (see, *e.g.*, (32)) that for these values of d , we have

$$H^2(\Omega) \subset C^0(\overline{\Omega}), \quad (1)$$

the injection of the Sobolev space $H^2(\Omega)$ into $C^0(\overline{\Omega})$ being *continuous* (in fact *compact*). Actually, many problems involving $H^2(\Omega)$ take place in (or make use of) the space $V := H^2(\Omega) \cap H_0^1(\Omega)$, a closed subspace of $H^2(\Omega)$ (12; 13; 14).

Since the injection from V into $C^0(\overline{\Omega})$ is continuous, there exists a positive constant C such that

$$\|\varphi\|_\infty \leq C \|\varphi\|_V, \quad \forall \varphi \in V, \quad (2)$$

with $\|\varphi\|_\infty = \max_{\mathbf{x} \in \overline{\Omega}} |\varphi(\mathbf{x})|$. The smallest constant C for which (2) holds is the norm of the above injection operator.

From now on (unless specified otherwise), we assume that Ω is *convex* and/or has a smooth boundary (denoted by $\Gamma = \partial\Omega$ in the sequel); if these properties hold, it follows from, *e.g.*, (23; 24) that the semi-norm $\varphi \rightarrow \|\Delta\varphi\|_{L^2(\Omega)}$ defines over V a norm equivalent to the norm induced by $H^2(\Omega)$. From this norm equivalence property, V is a Hilbert space for the scalar product $(v, w) \rightarrow \int_\Omega \Delta v \Delta w d\mathbf{x}$.

Let us denote by γ the *best* (that is the smallest) constant in (2). We have then (using the fact that the injection from V into $C^0(\overline{\Omega})$ is compact):

$$\gamma = \max_{\varphi \in \Sigma} \|\varphi\|_\infty \quad (3)$$

with $\Sigma = \left\{ \varphi \in V : \|\Delta\varphi\|_{L^2(\Omega)} = 1 \right\}$. The computation of γ is equivalent to solving a *non-smooth eigenvalue problem*. The main goal of this article is to discuss the numerical solution of the (kind of *non-linear bi-harmonic*) optimization problem (3). Two methods are considered: (i) the first one is obtained by combining a finite element approximation, a well chosen augmented Lagrangian, convex duality and variational methods for linear elliptic problems; (ii) the second method makes use of *Green's functions* and reduces the computation of γ to the solution of a d -dimensional constrained minimization problem. The solvability of the non-smooth eigenproblem is proved

in (25), where optimal constants are also given in various situations and the relation with Green's functions is emphasized (without the design of any numerical algorithms though). Related theoretical investigations can be found *e.g.* in (9; 15; 26; 27). Discussions of similar Sobolev or Sobolev-related inequalities can be found in (28; 37; 38)

The results of numerical experiments validate, in two dimensions, the computational methods discussed in this article. Comparisons with known exact solutions suggest that $|\gamma_h - \gamma| = \mathcal{O}(h^2)$, where γ_h is the discrete analogue of γ (obtained with a finite element discretization) and h a space discretization step.

Remark 1. If one replaces $\|\cdot\|_\infty$ by $\|\cdot\|_{L^2(\Omega)}$ in (3), then γ^{-1} is the square root of the smallest eigenvalue in the linear eigenproblem: find $u \in V \setminus \{0\}$ satisfying $\Delta^2 u = \lambda u$ in Ω , and $u = \Delta u = 0$ on Γ . From this observation, it is clear that the original problem (3) has some of the features of an eigenproblem, but the presence of $\|\cdot\|_\infty$ introduces a *non-smoothness* in (3).

Remark 2. Suppose that Γ is *non-smooth* and that Ω is *non-convex*. Assuming that Γ is Lipschitz continuous in the sense of Nečas (32), it may happen that Δ is still an isomorphism from $H^2(\Omega) \cap H_0^1(\Omega)$ onto $L^2(\Omega)$, but there are situations where this property is lost. As an illustration, let us consider Ω_1 and Ω_2 defined by

$$\Omega_1 = \left\{ \mathbf{x} = (x_1, x_2) \in \mathbb{R}^2, 0 < R_1 < \sqrt{x_1^2 + x_2^2} < R_2 < +\infty, x_2 > 0 \right\},$$

$$\Omega_2 = \left\{ \mathbf{x} = (x_1, x_2) \in \mathbb{R}^2, x_1 = r \cos \theta, x_2 = r \sin \theta, \right. \\ \left. 0 < r < R < +\infty, \pi/4 < \theta < 2\pi \right\}.$$

If $\Omega = \Omega_1$, Δ is still an isomorphism from $H^2(\Omega) \cap H_0^1(\Omega)$ onto $L^2(\Omega)$, but this is not true anymore if $\Omega = \Omega_2$. Actually, it still makes sense to look at problem (3) but, since Δ is not necessarily an isomorphism from $H^2(\Omega) \cap H_0^1(\Omega)$ onto $L^2(\Omega)$, one has to take for V the space $H(\Omega, \Delta) \cap H_0^1(\Omega)$, where $H(\Omega, \Delta) = \{v \in L^2(\Omega), \Delta v \in L^2(\Omega)\}$. As mentioned above, $H(\Omega, \Delta) \cap H_0^1(\Omega)$ can be larger than $H^2(\Omega) \cap H_0^1(\Omega)$; however, as shown by the results of numerical experiments, the methods discussed in this article have no particular difficulty at handling this more general situation.

Besides their purely mathematical interest, the best constants in Sobolev inequalities occur in at least three more applied areas, namely: (i) making more precise error estimates when performing, for example, finite element or finite difference approximations of partial

differential equations (8); (ii) identifying the domain of convergence of some parameter dependent iterative methods for the solution of partial differential equations (21); (iii) finding the time constants in the asymptotic behavior of the solutions of time dependent partial differential equations. As such, these best constants find applications in the mathematical and numerical analysis of a variety of equations from mathematical physics and mechanics. The equivalence between these constants and the results of constrained minimization or generalized eigenvalues problems also emphasizes this relation with applied problems from mechanics and physics. Non-smooth eigenvalue problems appear in continuum mechanics, for instance in the modeling of Bingham flows (3; 6), of elasto-plastic materials (4; 5), or in optimization of structures (36). Such non-differentiable functionals also arise in image processing (7; 19; 30) when designing denoising algorithms.

2. Some Exact Solutions

In order to validate the computational methods to be discussed in the following sections, we are going to investigate some situations where the exact value of γ can be obtained by analytical methods. Indeed, in some (simple) situations, the value of γ can be computed by using the closed form solution of the Laplace equation relying on Green's functions (11; 17). In that direction, we are going to prove the following result (see *e.g.* (31; 39)):

Theorem 1. *Suppose that $d = 1$ and $\Omega = (0, 1)$. We have then*

$$\gamma = \max_{\varphi \in \Sigma} \|\varphi\|_{\infty} = \frac{1}{4\sqrt{3}}. \quad (4)$$

Proof. Let us consider the following linear Dirichlet problem:

$$-\varphi''(x) = f(x), \quad x \in (0, 1), \quad \varphi(0) = \varphi(1) = 0,$$

with $f \in L^2(0, 1)$. This Dirichlet problem has a unique solution in $H^2(0, 1) \cap H_0^1(0, 1)$, given by

$$\varphi(x) = \int_0^1 G(x, y) f(y) dy, \quad \forall x \in [0, 1], \quad (5)$$

where $G(\cdot, \cdot)$ denotes the *Green's kernel* defined by

$$G(x, y) = \begin{cases} (1-x)y, & 0 \leq y \leq x, \\ x(1-y), & x \leq y \leq 1. \end{cases}$$

It follows from (5) and from the Schwarz inequality in $L^2(0, 1)$ that

$$|\varphi(x)| \leq \|f\|_{L^2(0,1)} \|G(x, \cdot)\|_{L^2(0,1)} \leq \|f\|_{L^2(0,1)} \max_{\xi \in [0,1]} \|G(\xi, \cdot)\|_{L^2(0,1)}. \quad (6)$$

It remains to compute the quantity $\max_{\xi \in [0,1]} \|G(\xi, \cdot)\|_{L^2(0,1)}$. Since

$$\|G(\xi, \cdot)\|_{L^2(0,1)}^2 = (1 - \xi)^2 \int_0^\xi y^2 dy + \xi^2 \int_\xi^1 (1 - y)^2 dy \leq \frac{1}{3} \frac{1}{16},$$

for all $\xi \in [0, 1]$, it follows from (6) that $|\varphi(x)| \leq \frac{1}{4\sqrt{3}} \|f\|_{L^2(0,1)}$. Since the above inequality is *sharp* (by taking $f(\cdot) = G(1/2, \cdot)$), it implies (4). \square

Theorem 2. *Suppose that $\Omega = \{(x_1, x_2) \in \mathbb{R}^2, x_1^2 + x_2^2 < 1\}$ ($d = 2$). We have then*

$$\gamma = \max_{\varphi \in \Sigma} \|\varphi\|_\infty = \frac{1}{2\sqrt{2\pi}}. \quad (7)$$

Proof. Let us consider the following elliptic problem

$$-\Delta u = f \quad \text{in } \Omega, \quad u = 0 \quad \text{on } \Gamma. \quad (8)$$

with $f \in L^2(\Omega)$. The Poisson-Dirichlet problem (8) has a unique solution in $H^2(\Omega) \cap H_0^1(\Omega)$, that is given by:

$$\varphi(\mathbf{x}) = \int_\Omega G(\mathbf{x}, \mathbf{y}) f(\mathbf{y}) d\mathbf{y}, \quad \forall \mathbf{x} \in \overline{\Omega}. \quad (9)$$

where the Green's function $\mathbf{y} \rightarrow G(\mathbf{x}, \mathbf{y})$ ($:= G(\mathbf{x}, \cdot)$) is the unique solution in $L^2(\Omega)$ of the following Dirichlet problem:

$$-\Delta G(\mathbf{x}, \cdot) = \delta_{(\mathbf{x})}(\cdot) \quad \text{in } \Omega, \quad G(\mathbf{x}, \cdot) = 0 \quad \text{on } \Gamma. \quad (10)$$

$\delta_{(\mathbf{x})}$ being the *Dirac measure* at \mathbf{x} . A *weak formulation* of (10) reads as follows: Find $G(\mathbf{x}, \cdot) \in L^2(\Omega)$ satisfying

$$-\int_\Omega G(\mathbf{x}, \cdot) \Delta v d\mathbf{y} = v(\mathbf{x}), \quad \forall v \in H^2(\Omega) \cap H_0^1(\Omega).$$

It follows from (9) and from the Schwarz inequality in $L^2(\Omega)$ that

$$|\varphi(\mathbf{x})| \leq \|f\|_{L^2(\Omega)} \|G(\mathbf{x}, \cdot)\|_{L^2(\Omega)} \leq \|f\|_{L^2(\Omega)} \sup_{\xi \in \Omega} \|G(\xi, \cdot)\|_{L^2(\Omega)}, \quad (11)$$

for all $\mathbf{x} \in \overline{\Omega}$. Assume that the supremum in (11) is in fact a maximum corresponding to $\boldsymbol{\xi} = (0, 0) =: \mathbf{0}$. Since for $\mathbf{x} = \mathbf{0}$ the solution of (10) (11; 17) is the function

$$\mathbf{y} \rightarrow G(\mathbf{0}, \mathbf{y}) = \frac{1}{2\pi} \ln \left(\frac{1}{|\mathbf{y}|} \right), \quad (12)$$

with $\mathbf{y} = (y_1, y_2)$, $|\mathbf{y}| = \sqrt{y_1^2 + y_2^2}$, the only thing left to estimate γ is to compute the $L^2(\Omega)$ -norm of the function in (12). Let us denote $|\mathbf{y}|$ by r ; we have then

$$\begin{aligned} \|G(\mathbf{0}, \cdot)\|_{L^2(\Omega)}^2 &= \frac{1}{4\pi^2} \int_{\Omega} \left[\ln \left(\frac{1}{|\mathbf{y}|} \right) \right]^2 d\mathbf{y} = \frac{1}{4\pi^2} \int_0^{2\pi} d\theta \int_0^1 \left[\ln \left(\frac{1}{r} \right) \right]^2 r dr \\ &= \frac{1}{2\pi} \int_0^1 \left[\ln \left(\frac{1}{r} \right) \right]^2 r dr = \frac{1}{2\pi} \int_0^{+\infty} t^2 e^{-2t} dt = \frac{1}{2\pi} \frac{1}{4}. \end{aligned}$$

This value, combined with (11), implies in turn that

$$|\varphi(\mathbf{x})| \leq \frac{1}{2\sqrt{2\pi}} \|f\|_{L^2(\Omega)}, \quad \forall \mathbf{x} \in \overline{\Omega}. \quad (13)$$

Since the inequality in (13) is sharp for $f = G(\mathbf{0}, \cdot)$, $\gamma = \frac{1}{2\sqrt{2\pi}}$. \square

Corollary 1. *Suppose now that Ω is the open unit ball of \mathbb{R}^3 centered at $\mathbf{0} = (0, 0, 0)$; a similar approach, relying on the fact that the optimal Green's function is again the function $\mathbf{y} \rightarrow G(\mathbf{0}, \mathbf{y})$ (with $G(\mathbf{0}, \mathbf{y}) = 1/(4\pi |\mathbf{y}|)$ here), we can show that $\gamma = 1/(2\sqrt{3\pi})$.*

When considering a two-dimensional domain that is not the unit disk, one can apply the same procedure, but an exact value is not available. For instance when considering the unit square $\Omega = (0, 1)^2$, the solution of (8) also reads $\varphi(\mathbf{x}) = \int_{\Omega} G(\mathbf{x}, \mathbf{y}) f(\mathbf{y}) d\mathbf{y}$, implying $|\varphi(\mathbf{x})| \leq \|f\|_{L^2(\Omega)} \|G(\mathbf{x}, \cdot)\|_{L^2(\Omega)}$. Let us assume that the optimal Green's function is the function $\mathbf{y} \rightarrow G(\mathbf{C}, \mathbf{y})$, where $\mathbf{C} = (1/2, 1/2)$ is the center of the square. The solution of the elliptic problem for the Green's kernel:

$$-\Delta G(\mathbf{C}, \cdot) = \delta_{(\mathbf{C})}(\cdot), \quad \text{in } \Omega, \quad G(\mathbf{C}, \cdot) = 0, \quad \text{on } \Gamma.$$

is given by $G(\mathbf{C}, \mathbf{x}) = \frac{1}{2\pi} \ln \left(\frac{1}{|\mathbf{C} - \mathbf{x}|} \right) + u_0(\mathbf{x})$, where

$$-\Delta u_0(\mathbf{x}) = 0, \quad \mathbf{x} \in \Omega, \quad u_0(\mathbf{x}) = -\frac{1}{2\pi} \ln \left(\frac{1}{|\mathbf{x} - \mathbf{C}|} \right), \quad \mathbf{x} \in \Gamma. \quad (14)$$

Following the same strategy as in the previous case, we have:

$$\gamma = \|G(\mathbf{C}, \cdot)\|_{L^2(\Omega)} = \left\| \frac{1}{2\pi} \ln \left(\frac{1}{|\mathbf{C} - \cdot|} \right) + u_0(\cdot) \right\|_{L^2(\Omega)}. \quad (15)$$

Solving (14) numerically allows to obtain an approximation of u_0 and compute γ in (15) with numerical quadrature formulas.

3. Two Strategies for the Computation of the Best Constant γ

In order to compute γ , two strategies appear quite clearly, namely:

- (i) **A Green's function based strategy.** This approach relies on the statement, implied by the developments in Sections 1 and 2, that the function $\varphi \in H^2(\Omega) \cap H_0^1(\Omega)$ satisfying the optimum γ on the domain Ω is the function solution of the following minimization problem:

$$\sup_{\mathbf{x}_0 \in \overline{\Omega}} \|G(\mathbf{x}_0, \cdot)\|_{L^2(\Omega)}, \quad (16)$$

where $-\Delta G(\mathbf{x}_0, \cdot) = \delta_{(\mathbf{x}_0)}(\cdot)$ in Ω , $G(\mathbf{x}_0, \cdot) = 0$ on Γ . This property of the best constant γ relying on Green's functions has already been highlighted in (25), without discussing any numerical procedure. This approach is discussed in Section 4.

- (ii) **An augmented Lagrangian based strategy.** This methodology relying on duality arguments, is discussed more extensively in Section 5. Although it looks more complicated than the approach based on Green's functions, it is easier to implement, since it involves only classical optimization techniques.

4. A Green's Function Based Strategy

The notation and the hypotheses on Ω are the same as in Sections 1 and 2. To $f \in L^2(\Omega)$, we associate the unique solution in $H^2(\Omega) \cap H_0^1(\Omega)$ of the Dirichlet problem

$$-\Delta \varphi = f \text{ in } \Omega, \quad \varphi = 0 \text{ on } \Gamma. \quad (17)$$

We have then, as in Section 2,

$$|\varphi(\mathbf{x})| \leq \|G(\mathbf{x}, \cdot)\|_{L^2(\Omega)} \|f\|_{L^2(\Omega)} \leq \sup_{\boldsymbol{\xi} \in \Omega} \|G(\boldsymbol{\xi}, \cdot)\|_{L^2(\Omega)} \|f\|_{L^2(\Omega)}, \quad (18)$$

for all $\mathbf{x} \in \overline{\Omega}$, where, G is the Green's function associated with the Poisson-Dirichlet problem (17). This means that the function $\mathbf{y} \rightarrow G(\mathbf{x}, \mathbf{y})$ is the unique solution in $L^2(\Omega)$ of the Dirichlet problem

$$-\Delta G(\mathbf{x}, \cdot) = \delta_{(\mathbf{x})}, \quad \text{in } \Omega, \quad G(\mathbf{x}, \cdot) = 0, \quad \text{on } \Gamma, \quad (19)$$

$\delta_{(\mathbf{x})}$ being the *Dirac measure* at \mathbf{x} . The inequality in (18) being sharp, in order to compute γ , we have to solve the following constrained d -dimensional optimization problem

$$\max_{\mathbf{X} \in \overline{\Omega}} \|G(\mathbf{X}, \cdot)\|_{L^2(\Omega)}, \quad (20)$$

$G(\mathbf{X}, \cdot)$ being the solution of problem (19) with $\mathbf{x} = \mathbf{X}$. The optimization problem (20) being of low dimension, it is possible to apply to its solution those derivative-free optimization methods discussed in, *e.g.*, (2; 10; 34) (see also the references therein); for some situations, symmetry considerations allow to reduce the dimension of the feasible solutions set. For those willing to make use of derivatives, let us observe that problem (20) is equivalent to:

$$\max_{\mathbf{X} \in \overline{\Omega}} J(\mathbf{X}), \quad \text{where} \quad J(\mathbf{X}) = \frac{1}{2} \int_{\Omega} g^2 d\mathbf{x},$$

the function g being the unique solution in $L^2(\Omega)$ of

$$-\Delta g = \delta_{(\mathbf{X})} \quad \text{in } \Omega, \quad g = 0 \quad \text{on } \Gamma.$$

A *weak formulation* of this problem is: Find $g \in L^2(\Omega)$ such that

$$-\int_{\Omega} g \Delta v d\mathbf{x} = v(\mathbf{X}), \quad \forall v \in H^2(\Omega) \cap H_0^1(\Omega). \quad (21)$$

In order to compute the differential $DJ(\mathbf{X})$ of the functional J at \mathbf{X} , we use a classical *perturbation analysis* (as done in (20)). Let us denote by $\delta\mathbf{X}$ a perturbation of \mathbf{X} , and by δg and δJ the corresponding variations of g and J . We have then

$$\delta J(\mathbf{X}) = DJ(\mathbf{X}) \cdot \delta\mathbf{X} = \int_{\Omega} g \delta g d\mathbf{x},$$

where, with obvious notation, $\mathbf{Y} \cdot \mathbf{Z} = \sum_{j=1}^d Y_j Z_j$ and, from (21),

$$-\int_{\Omega} \delta g \Delta v d\mathbf{x} = \nabla v(\mathbf{X}) \cdot \delta \mathbf{X}, \quad \forall v \in H^2(\Omega) \cap H_0^1(\Omega) \cap C^1(\overline{\Omega}). \quad (22)$$

Let us define p as the unique solution in $H^2(\Omega) \cap H_0^1(\Omega)$ of (the adjoint problem):

$$-\Delta p = g \quad \text{in } \Omega, \quad p = 0 \quad \text{on } \Gamma,$$

If $d = 1$ or 2 , p has enough regularity to belong to $C^1(\overline{\Omega})$, which implies that one can take $v = p$ in (22); if we do so, combining the above relations shows that:

$$DJ(\mathbf{X}) = \nabla p(\mathbf{X}), \quad \forall \mathbf{X} \in \Omega.$$

If $\bar{\mathbf{X}}$ minimizes J over the open set Ω , we have $\nabla p(\bar{\mathbf{X}}) = 0$. For $\mathbf{X}^0 \in \Omega$ given, we can construct an iterative sequence $\{\mathbf{X}^k\}_{k \geq 0}$ that eventually converges to $\bar{\mathbf{X}}$ that is the maximizer of (20). This iterative algorithm reads as follows.

$$\mathbf{X}^{k+1} = \mathbf{X}^k + \alpha_k DJ(\mathbf{X}^k) = \mathbf{X}^k + \alpha_k \nabla p(\mathbf{X}^k),$$

where α_k is a *step-length*, and $DJ(\mathbf{X}^k)$ is the *search direction*.

A finite element implementation of this algorithm is given in Section 7. Numerical results obtained with this approach are given in Section 8, mainly to validate the (more efficient) *augmented Lagrangian based strategy*.

5. An Augmented Lagrangian Based Strategy

5.1. A Saddle-Point Formulation

Let Ω be a bounded domain of \mathbb{R}^d , $d = 2, 3$, such that Ω is convex and/or $\Gamma = \partial\Omega$ is smooth. We consider the following optimization problem:

$$\gamma = \max_{\varphi \in \Sigma} \|\varphi\|_{\infty}, \quad (23)$$

with $\Sigma = \left\{ \varphi \in H^2(\Omega) \cap H_0^1(\Omega) : \|\Delta\varphi\|_{L^2(\Omega)} = 1 \right\}$. We observe that

$$\gamma = \max_{\varphi \in \Sigma} \|\varphi\|_{\infty} = \max_{(\varphi, \mu) \in \Sigma \times \Lambda} \langle \mu, \varphi \rangle, \quad (24)$$

where $\Lambda = \left\{ \mu \in \mathcal{M}_b : \|\mu\|_{\mathcal{M}_b} \leq 1 \right\}$. The quantities appearing in (24) are defined as follows:

- (i) \mathcal{M}_b is the dual space of $C_0^0(\overline{\Omega}) = \{\varphi \in C^0(\overline{\Omega}) : \varphi = 0 \text{ on } \Gamma\}$, equipped with the $\|\cdot\|_\infty$ -norm; $C_0^0(\overline{\Omega})$ is a *Banach space*;
- (ii) $\langle \cdot, \cdot \rangle$ is the duality pairing between \mathcal{M}_b and $C_0^0(\overline{\Omega})$, which verifies $\langle f, \varphi \rangle = \int_{\Omega} f\varphi d\mathbf{x}$, for all $f \in L^1(\Omega)$ and $\varphi \in C_0^0(\overline{\Omega})$.
- (iii) $\|\mu\|_{\mathcal{M}_b}$ is (classically) defined by $\|\mu\|_{\mathcal{M}_b} = \sup_{\varphi \in C_0^0(\overline{\Omega}) \setminus \{0\}} \frac{|\langle \mu, \varphi \rangle|}{\|\varphi\|_\infty}$.
- (iv) $L^1(\Omega) \subset \mathcal{M}_b$.
- (v) $\delta_{(\mathbf{x})} \in \Lambda$, for all $x \in \Omega$, and $\|\delta_{(\mathbf{x})}\|_{\mathcal{M}_b} = 1$, for all $\mathbf{x} \in \Omega$.

The space \mathcal{M}_b is known as the *space of the bounded Radon measures* over $C_0^0(\overline{\Omega})$. Actually, we can reduce the set where one is looking for a solution of problem (23) by observing that if ψ is a solution of (23), then $-\psi$ is also solution and there exists $\mathbf{X} \in \Omega$ such that

$$\begin{aligned} -\Delta\psi &= \pm \frac{G(\mathbf{X}, \cdot)}{\|G(\mathbf{X}, \cdot)\|_{L^2(\Omega)}} \quad \text{in } \Omega, \psi = 0 \quad \text{on } \Gamma, \\ -\Delta G(\mathbf{X}, \cdot) &= \delta_{(\mathbf{X})} \quad \text{in } \Omega, G(\mathbf{X}, \cdot) = 0 \quad \text{on } \Gamma, \end{aligned}$$

The positivity of $\delta_{(\mathbf{X})}$ (in the sense of measures) and the *maximum principle* for second order elliptic operators (see, *e.g.*, (17)) imply that $G(\mathbf{X}, \cdot) \geq 0$, *a.e.* in Ω , which implies (again from the maximum principle) that either $\psi \geq 0$ or $\psi \leq 0$.

From now on, we focus on the non-negative solutions of problem (23). A simple way to reach that goal is to replace Σ by

$$\Sigma^+ = \{\varphi \in \Sigma : -\Delta\varphi \geq 0 \text{ a.e. in } \Omega\}.$$

In a similar way, if $\psi \geq 0$ is a solution of (23) reaching its maximum value at $\mathbf{x} = \mathbf{X}$, we have $\max_{\varphi \in \Sigma} \|\varphi\|_\infty = \psi(\mathbf{X}) = \langle \delta_{(\mathbf{X})}, \psi \rangle = \max_{(\varphi, \mu) \in \Sigma \times \Lambda} \langle \mu, \varphi \rangle$, a relation which suggests to restrict our search to those elements of Λ which are also *positive measures* (as is $\delta_{(\mathbf{X})}$), *i.e.* which belong to

$$\Lambda^+ = \{\mu \in \Lambda : \langle \mu, \varphi \rangle \geq 0, \forall \varphi \in C_0^0(\overline{\Omega}), \varphi \geq 0\}.$$

From the above facts, an equivalent formulation of the original problem reads as follows:

$$\min_{(\varphi, \mu) \in \Sigma^+ \times \Lambda^+} - \langle \mu, \varphi \rangle, \quad (25)$$

The main difficulty with this problem comes from the two constraints verified by $\Delta\varphi$, namely $\|\Delta\varphi\|_{L^2(\Omega)} = 1$ and $-\Delta\varphi \geq 0$, giving to (25) the features of a *nonlinear bi-harmonic problem*. In order to overcome this difficulty, we observe that there is equivalence between (25) and

$$\min_{((v,z,\varphi),\mu)\in\mathcal{E}\times\Lambda^+} -\langle \mu, \varphi \rangle, \quad (26)$$

the set \mathcal{E} being defined by

$$\mathcal{E} = \left\{ v \in L^2(\Omega), z \in L^2(\Omega), \varphi \in H^2(\Omega) \cap H_0^1(\Omega) : \right. \\ \left. -\Delta\varphi = v \text{ in } \Omega, z \geq 0, \|z\|_{L^2(\Omega)} = 1, v - z = 0 \right\}.$$

We associate with (26) the augmented Lagrangian functional \mathcal{L}_r defined, with $r > 0$, by

$$\mathcal{L}_r(v, \varphi, z, \mu, m) = -\langle \mu, \varphi \rangle + \frac{r}{2} \int_{\Omega} |v - z|^2 d\mathbf{x} + \int_{\Omega} m(v - z) d\mathbf{x}. \quad (27)$$

We consider the *saddle-point problem*: find $(u, \psi) \in \mathcal{U}$, $y \in \mathcal{S}_2^+$, $\lambda \in \Lambda^+$, $\ell \in L^2(\Omega)$, such that

$$\mathcal{L}_r(u, \psi, y, \lambda, m) \leq \mathcal{L}_r(u, \psi, y, \lambda, \ell) \leq \mathcal{L}_r(v, \varphi, z, \mu; \ell), \quad (28)$$

for all $(v, \varphi) \in \mathcal{U}$, $z \in \mathcal{S}_2^+$, $\mu \in \Lambda^+$, $m \in L^2(\Omega)$, with

$$\mathcal{U} = \left\{ (v, \varphi) \in L^2(\Omega) \times H^2(\Omega) \cap H_0^1(\Omega) : -\Delta\varphi = v \text{ in } \Omega \right\}, \\ \mathcal{S}_2^+ = \left\{ z \in L^2(\Omega) : z \geq 0, \|z\|_{L^2(\Omega)} = 1 \right\}.$$

If the saddle-point problem has a solution we can show that $y = u = -\Delta\psi$, with $\psi \in \Sigma^+$. Moreover, it follows from the second inequality in (28), that $\langle \lambda, \psi \rangle = \max_{(\mu, \varphi) \in \Lambda^+ \times \Sigma^+} \langle \mu, \varphi \rangle = \max_{\varphi \in \Sigma} \|\varphi\|_{\infty}$. From the definition of Λ , we have $\|\lambda\|_{\mathcal{M}_b} \leq 1$, since $\lambda \in \Lambda^+ \subset \Lambda$; it follows then that $\|\psi\|_{\infty} = \max_{\varphi \in \Sigma} \|\varphi\|_{\infty}$, which implies that ψ is a solution of problem (23).

5.2. An Iterative Method

To solve the saddle-point problem (28), we advocate the algorithm ALG2 discussed in (18; 22); when applied to the solution of (28), this *Douglas-Rachford-Uzawa algorithm* reads as follows:

$$(y^{-1}, \lambda^{-1}, \ell^0) \text{ is given in } \mathcal{S}_2^+ \times \Lambda^+ \times L^2(\Omega). \quad (29)$$

For instance, one can choose $y^{-1} = 1/\sqrt{|\Omega|}$, $\lambda^{-1} = 1/|\Omega|$, $\ell^0 = 0$, where $|\Omega|$ is the measure of Ω . Then, for $n \geq 0$, we assume that y^{n-1} , λ^{n-1} and ℓ^n are known and we proceed as follows to compute y^n , ψ^n , y^n , λ^n and ℓ^{n+1} :

(a) Solve

$$(u^n, \psi^n) = \arg \min_{(v, \varphi) \in \mathcal{U}} \mathcal{L}_r(v, \varphi, y^{n-1}, \lambda^{n-1}, \ell^n). \quad (30)$$

(b) Solve

$$y^n = \arg \min_{z \in \mathcal{S}_2^+} \mathcal{L}_r(u^n, \psi^n, z, \lambda^{n-1}, \ell^n). \quad (31)$$

(c) Solve

$$\lambda^n = \arg \min_{\mu \in \Lambda^+} \mathcal{L}_r(u^n, \psi^n, y^n, \mu, \ell^n). \quad (32)$$

(d) Update the multipliers $\ell^n \in L^2(\Omega)$ via:

$$\ell^{n+1} = \ell^n + r(u^n - y^n), \quad (33)$$

until convergence is reached.

Typically the stopping criterion is $\|\psi^n - \psi^{n-1}\|_{L^2(\Omega)} < \varepsilon$, where ε is a given tolerance. The solution of the sub-problems encountered in (a), (b) and (c) are discussed in the three following subsections; among these three sub-problems, the most costly to solve is definitely (30), while the most 'exotic' one is (32).

5.3. On the Solution of Problem (30)

Let $X^n := ry^{n-1} - \ell^n \in L^2(\Omega)$. It follows from (27) that problem (30) reduces to

$$\min_{(v, \varphi) \in \mathcal{U}} - \langle \lambda^{n-1}, \varphi \rangle + \frac{r}{2} \int_{\Omega} |v|^2 d\mathbf{x} - \int_{\Omega} X^n v d\mathbf{x}.$$

Since $v = -\Delta\varphi$, this problem is equivalent to

$$\min_{\varphi \in H^2(\Omega) \cap H_0^1(\Omega)} - \langle \lambda^{n-1}, \varphi \rangle + \frac{r}{2} \int_{\Omega} |\Delta\varphi|^2 d\mathbf{x} + \int_{\Omega} X^n \Delta\varphi d\mathbf{x}.$$

Using convex analysis arguments (see, *e.g.*, (16; 29)), one can show that this problem has a unique solution $\psi^n \in H^2(\Omega) \cap H_0^1(\Omega)$ characterized by

$$r \int_{\Omega} \Delta\psi^n \Delta\varphi d\mathbf{x} = \langle \lambda^{n-1}, \varphi \rangle - \int_{\Omega} X^n \Delta\varphi d\mathbf{x}, \quad \forall \varphi \in H^2(\Omega) \cap H_0^1(\Omega). \quad (34)$$

Let us define p^{n-1} as the unique solution in $L^2(\Omega)$ of the following Dirichlet problem

$$-\Delta p^{n-1} = \lambda^{n-1} \text{ in } \Omega, \quad p^{n-1} = 0 \text{ on } \Gamma. \quad (35)$$

A weak formulation of (35) is given by: find $p^{n-1} \in L^2(\Omega)$ satisfying $-\int_{\Omega} p^{n-1} \Delta \varphi d\mathbf{x} = \langle \lambda^{n-1}, \varphi \rangle$, for all $\varphi \in H^2(\Omega) \cap H_0^1(\Omega)$. Using this last relation, (34) becomes

$$r \int_{\Omega} \Delta \psi^n \Delta \varphi d\mathbf{x} = - \int_{\Omega} (X^n + p^{n-1}) \Delta \varphi d\mathbf{x}, \quad \forall \varphi \in H^2(\Omega) \cap H_0^1(\Omega).$$

Since Δ is an isomorphism from $H^2(\Omega) \cap H_0^1(\Omega)$ onto $L^2(\Omega)$, this relation implies $-\Delta \psi^n = \frac{1}{r} (X^n + p^{n-1})$, and $\psi^n \in H^2(\Omega) \cap H_0^1(\Omega)$. Therefore the solution of problem (30) is clearly (u^n, ψ^n) with $u^n = \frac{1}{r} (X^n + p^{n-1})$. Let us summarize: in order to compute the pair (u^n, ψ^n) solution of (30), we compute first the solution p^{n-1} of the Dirichlet problem (35). We have then $u^n = \frac{1}{r} (X^n + p^{n-1})$, and finally ψ^n is obtained as the unique solution in $H^2(\Omega) \cap H_0^1(\Omega)$ of the Dirichlet problem $-\Delta \psi^n = u^n$ in Ω .

5.4. On the Solution of the Problem (31)

Let $Y^n = ru^n + \ell^n$. It follows from (27) that (31) reduces to

$$\min_{z \in \mathcal{S}_2^+} \frac{r}{2} \int_{\Omega} |z|^2 d\mathbf{x} - \int_{\Omega} z Y^n d\mathbf{x}. \quad (36)$$

Since $z \in \mathcal{S}_2^+$ and $\int_{\Omega} |z|^2 d\mathbf{x} = 1$, problem (36) further simplifies, reducing to

$$\min_{z \in \mathcal{S}_2^+} - \int_{\Omega} Y^n z d\mathbf{x} = - \max_{z \in \mathcal{S}_2^+} \int_{\Omega} Y^n z d\mathbf{x}.$$

Suppose that $(Y^n)^+ := \sup(0, Y^n) \neq 0$; it follows then from the Schwarz inequality in $L^2(\Omega)$ that the solution y^n of problem (31) is given by $y^n = (Y^n)^+ / \|(Y^n)^+\|_{L^2(\Omega)}$. If $(Y^n)^+ = 0$, take for y^n an arbitrary element of \mathcal{S}_2^+ .

Remark 3. To tell the truth, when applying algorithm (29)-(32) (actually its discrete analogue described in Section 6.3), initialized with $y^{-1} = 1/\sqrt{|\Omega|}$, $\lambda^{-1} = 1/|\Omega|$, and $\ell^0 = 0$, to the solution of the test problems considered in Section 8, we never encountered the case $(Y^n)^+ = 0$.

5.5. On the Solution of Problem (32)

Problem (32) reduces to

$$\min_{\mu \in \Lambda^+} - \langle \mu, \psi^n \rangle = - \max_{\mu \in \Lambda^+} \langle \mu, \psi^n \rangle .$$

The function ψ^n being continuous over $\overline{\Omega}$, it reaches its maximum value at \mathbf{x}_0^n (ψ^n may have other maximizers than \mathbf{x}_0^n). We have the closed form solution:

$$\lambda^n = \begin{cases} \delta_{(\mathbf{x}_0^n)}, & \text{if } \psi^n(\mathbf{x}_0^n) > 0, \\ 0, & \text{if } \psi^n(\mathbf{x}_0^n) = 0. \end{cases}$$

6. Finite Element Implementation of the Augmented Lagrangian Based Strategy

6.1. Generalities

We suppose from now on that Ω is a bounded domain of \mathbb{R}^2 . In order to solve (23) via finite element techniques, we introduce first a family $\{\Omega_h\}_h$ of polygonal domains of \mathbb{R}^2 (approximations of the domain Ω), such that $\lim_{h \rightarrow 0} \Omega_h = \Omega$ and $\lim_{h \rightarrow 0} \Gamma_h = \Gamma$, where $\Gamma_h = \partial\Omega_h$. More precisely, by $\lim_{h \rightarrow 0} \Omega_h = \Omega$, we mean that:

- (a) If O is an open subset of \mathbb{R}^2 such that $\overline{\Omega} \subset O$, then $\overline{\Omega}_h \subset O$ for all $h > 0$ sufficiently small.
- (b) If K is a compact subset of Ω , then $K \subset \Omega_h$ for all $h > 0$ sufficiently small.

Further details concerning the approximation of Γ by $\{\Gamma_h\}_h$ are given below. Next we consider a family $\{\mathcal{T}_h\}_h$ of triangulations of Ω_h , verifying the following (classical) assumptions (see, *e.g.*, (8)), that is

- (i) All the triangles T of \mathcal{T}_h are closed, and $\bigcup_{T \subset \mathcal{T}_h} T = \overline{\Omega}_h$.
- (ii) If T_1 and T_2 belong to \mathcal{T}_h then either $T_1 \cap T_2 = \emptyset$, or T_1 and T_2 have only a vertex in common or only a full edge in common.

- (iii) h is the length of the largest edge(s) of \mathcal{T}_h .
- (iv) If θ_h is the smallest angle of \mathcal{T}_h , then $\inf_h \theta_h > 0$.
- (v) All the vertices of \mathcal{T}_h located on Γ_h belong to Γ .

Let \mathbb{P}_k be the space of polynomials of degree less than or equal to k . As usual, we approximate $H^1(\Omega)$ and $H_0^1(\Omega)$ using, respectively, $\{V_h\}_h$ and $\{V_{0,h}\}_h$, two families of *finite element spaces* defined by

$$V_h = \{v \in C^0(\overline{\Omega}_h) : v|_T \in \mathbb{P}_1, \forall T \in \mathcal{T}_h\}, \quad (37)$$

$$V_{0,h} = \left\{v \in V_h : v|_{\Gamma_h} = 0\right\}. \quad (38)$$

Let φ_j , $j = 1, \dots, N_n$ be the finite element basis functions of $V_{0,h}$, based on the triangulation \mathcal{T}_h . Since $C_0^0(\overline{\Omega}) \subset L^2(\Omega) \subset \mathcal{M}_b$ and $H_0^1(\Omega) \subset L^2(\Omega) \subset \mathcal{M}_b$, with *continuity* of the injections and *density* of the inclusions (possibly in the weak- \star sense), it makes sense to use the family $\{V_{0,h}\}_h$ to approximate simultaneously $H_0^1(\Omega)$, $C_0^0(\overline{\Omega})$, $L^2(\Omega)$ and \mathcal{M}_b . As we will see in Section 6.2, such a choice simplifies considerably the approximation of (23). In order to further simplify the approximation of (23), we approximate over $V_{0,h}$ the scalar product of $L^2(\Omega)$, and the corresponding norm, by

$$(v, w)_{0,h} = \frac{1}{3} \sum_{j=1}^{N_{0h}} A_j v(P_j) w(P_j), \quad \|v\|_{0,h} = \sqrt{(v, v)_{0,h}},$$

for all $v, w \in V_{0,h}$, where (i) $\{P_j\}_{j=1}^{N_{0h}}$ is the set of the vertices of \mathcal{T}_h which do not belong to Γ_h and N_{0h} is the dimension of $V_{0,h}$; (ii) A_j is the measure of the polygonal which is the union of those triangles of \mathcal{T}_h having P_j as a common vertex, implying that the scalar product $(\cdot, \cdot)_{0,h}$ is the approximation of the $L^2(\Omega)$ -scalar product obtained by applying the *trapezoidal rule* on each triangle of \mathcal{T}_h .

6.2. Definition of the Approximate Problem

It follows from Section 5 that the *maximum principle* for second order elliptic operators plays an important role when restricting our search to non-negative solutions and taking -in some sense- $v = -\Delta\varphi$ as the master unknown function. In order to ensure that the discrete analogue of $-\Delta$ also verifies a maximum principle, we complete the properties (i)-(v) verified by $\{\mathcal{T}_h\}_h$ by the following one:

- (vi) For all h , the angles of \mathcal{T}_h are $\leq \frac{\pi}{2}$.

Condition (vi) is a *sufficient condition* to impose a discrete maximum principle when using -as we do- piecewise affine finite element approximations (cf. (8)). Another nice property of the finite element spaces we employ is that if $v \in V_h$, V_h being defined by (37), v reaches its maximum value at a vertex of \mathcal{T}_h (possibly at several).

Of the several equivalent formulations of problem (23) that we considered in Section 5, the one we are going to approximate is (25). The *discrete problem* that we consider is thus:

$$\min_{((v,\varphi),\mu) \in \Sigma_h^+ \times \Lambda_h^+} -(\mu, \varphi)_{0,h}, \quad (39)$$

with

$$\Sigma_h^+ = \left\{ (v, \varphi) \in (V_{0,h})^2 : \int_{\Omega_h} \nabla \varphi \cdot \nabla \theta d\mathbf{x} = (v, \theta)_{0,h}, \forall \theta \in V_{0,h}, \right. \\ \left. v \geq 0, (v, v)_{0,h} = 1 \right\}$$

and

$$\Lambda_h^+ = \left\{ \mu \in V_{0,h} : \mu(P_j) \geq 0, \forall j = 1, \dots, N_{0h}, \frac{1}{3} \sum_{j=1}^{N_{0h}} A_j \mu(P_j) \leq 1 \right\}.$$

Problem (39) is clearly equivalent to

$$\min_{((v,z,\varphi),\mu) \in \mathcal{E}_h \times \Lambda_h^+} -(\mu, \varphi)_{0,h}, \quad (40)$$

where

$$\mathcal{E}_h = \left\{ (v, z, \varphi) \in (V_{0,h})^3 : \int_{\Omega_h} \nabla \varphi \cdot \nabla \theta d\mathbf{x} = (v, \theta)_{0,h}, \forall \theta \in V_{0,h}, \right. \\ \left. z(P_j) \geq 0, \forall j = 1, \dots, N_{0h}, (z, z)_{0,h} = 1, v - z = 0 \right\}.$$

Guided by the continuous problem (see Section 5.1), we associate with the minimization problem (40) the following augmented Lagrangian functional:

$$\mathcal{L}_{hr}(v, \varphi, z, \mu, m) = -(\mu, \varphi)_{0,h} + \frac{r}{2}(v - z, v - z)_{0,h} + (m, v - z)_{0,h} \quad (41)$$

and the discrete saddle-point problem reads: find $(u_h, \psi_h) \in \mathcal{U}_h$, $y_h \in \mathcal{S}_{2h}^+$, $\lambda_h \in \Lambda_h^+$, $\ell_h \in V_{0,h}$, such that

$$\begin{aligned} \mathcal{L}_{hr}(u_h, \psi_h, y_h, \lambda_h, m_h) &\leq \mathcal{L}_{hr}(u_h, \psi_h, y_h, \lambda_h, \ell_h) \\ &\leq \mathcal{L}_{hr}(v_h, \varphi_h, z_h, \mu_h, \ell_h), \end{aligned} \quad (42)$$

for all $(v_h, \varphi_h) \in \mathcal{U}_h$, $z_h \in \mathcal{S}_{2h}^+$, $\mu_h \in \Lambda_h^+$, $m_h \in V_{0,h}$, with

$$\begin{aligned} \mathcal{U}_h &= \left\{ (v, \varphi) \in V_{0,h} \times V_{0,h} : \int_{\Omega_h} \nabla \varphi \cdot \nabla \theta d\mathbf{x} = (v, \theta)_{0,h}, \forall \theta \in V_{0,h} \right\}, \\ \mathcal{S}_{2h}^+ &= \{z \in V_{0,h} : z(P_j) \geq 0, \forall j = 1, \dots, N_{0h}, (z, z)_{0,h} = 1\}. \end{aligned}$$

Suppose that $(u_h, \psi_h, y_h, \lambda_h, \ell_h)$ is a solution of the saddle-point problem (42); we have then $u_h = y_h \geq 0$ and $u_h = y_h \neq 0$, which implies that the solution $\psi_h \in V_{0,h}$ of the following discrete Dirichlet problem: $\int_{\Omega_h} \nabla \psi_h \cdot \nabla \theta d\mathbf{x} = (u_h, \theta)_{0,h}$, for all $\theta \in V_{0,h}$, is different from zero and (by the discrete maximum principle) strictly positive in Ω_h . These properties imply that ψ_h reaches its (necessarily strictly positive) maximum values at some vertex of \mathcal{T}_h not located on Γ_h , that is there exists $i_0 \in \{1, \dots, N_{0h}\}$ such that $\psi_h(P_{i_0}) = |\psi_h(P_{i_0})| = \|\psi_h\|_\infty$. On the other hand, it follows from (42) that

$$\|\psi_h\|_\infty \geq (\lambda_h, \psi_h)_{0,h} = \max_{((v,\varphi),\mu) \in \mathcal{U}_h \times \Lambda_h^+} (\mu, \varphi)_{0,h} \geq (\mu, \psi_h)_{0,h}, \forall \mu \in \Lambda_h^+.$$

In the previous relation, let us take for the test function μ the element λ_{i_0} of Λ_h^+ (an approximation of the Dirac measure at P_{i_0}) defined by $\lambda_{i_0} = (3/A_{i_0})w_{i_0}$, where w_{i_0} is the unique element of $V_{0,h}$ verifying

$$w_{i_0}(P_j) = \begin{cases} 1, & \text{when } j = i_0, \\ 0, & \forall j = 1, \dots, N_{0h}, j \neq i_0. \end{cases}$$

We have then $\|\psi_h\|_\infty \geq (\lambda_h, \psi_h)_{0,h} \geq (\lambda_{i_0}, \psi_h)_{0,h} = \psi_h(P_{i_0}) = |\psi_h(P_{i_0})| = \|\psi_h\|_\infty$, implying that at the discrete level $\gamma_h = (\lambda_h, \psi_h)_{0,h}$ mimics the property of γ in the continuous case.

6.3. Iterative Solution of the Discrete Saddle Point Problem

6.3.1. Description of the Algorithm Inspired by the continuous case, we solve (39) by applying the *Douglas-Rachford-Uzawa algorithm* ALG2 to the solution of the saddle-point problem (42). The resulting algorithm reads as follows:

$$(y_h^{-1}, \lambda_h^{-1}, \ell_h^0) \text{ is given in } \mathcal{S}_{2h}^+ \times \Lambda_h^+ \times V_{0,h}; \quad (43)$$

for instance, one can choose $(y_h^{-1}, \lambda_h^{-1}, \ell_h^0) \in (V_{0,h})^3$ such that $y_h^{-1}(P_j) = 1/\sqrt{|\Omega_h|}$, $\lambda_h^{-1}(P_j) = 1/|\Omega_h|$, for all $j = 1, \dots, N_{0h}$, $\ell_h^0 = 0$. Then, for $n \geq 0$, we assume that y_h^{n-1} , λ_h^{n-1} , and ℓ_h^n are known, and we proceed as follows to compute u_h^n , ψ_h^n , y_h^n , λ_h^n and ℓ_h^{n+1} :

(a) Solve

$$(u_h^n, \psi_h^n) = \arg \min_{(v, \varphi) \in \mathcal{U}_h} \mathcal{L}_{hr}(v, \varphi, y_h^{n-1}, \lambda_h^{n-1}, \ell_h^n). \quad (44)$$

(b) Solve

$$y_h^n = \arg \min_{z \in \mathcal{S}_{2h}^+} \mathcal{L}_{hr}(u_h^n, \psi_h^n, z, \lambda_h^{n-1}, \ell_h^n). \quad (45)$$

(c) Solve

$$\lambda_h^n = \arg \min_{\mu \in \Lambda_h^+} \mathcal{L}_{hr}(u_h^n, \psi_h^n, y_h^n, \mu, \ell_h^n). \quad (46)$$

(d) Update the multipliers $\ell_h^n \in V_{0,h}$ as follows:

$$\ell_h^{n+1} = \ell_h^n + r(u_h^n - y_h^n), \quad (47)$$

until convergence is reached. Typically the stopping criterion is $\|\psi_h^n - \psi_h^{n-1}\|_{0,h} < \varepsilon$, where ε is a given tolerance. The solution of the sub-problems encountered in (a), (b) and (c) are discussed in the following subsections.

6.3.2. On the Solution of Problem (44) Let $X_h^n := ry_h^{n-1} - \ell_h^n \in V_{0,h}$. It follows from (41) that problem (44) reduces to

$$\min_{(v, \varphi) \in \mathcal{U}_h} -(\lambda_h^{n-1}, \varphi)_{0,h} + \frac{r}{2}(v, v)_{0,h} - (X_h^n, v)_{0,h}.$$

Using convexity arguments, one can show that it has a unique solution $(u_h^n, \psi_h^n) \in \mathcal{U}_h$ characterized by

$$r(u_h^n, v)_{0,h} = (X_h^n, v)_{0,h} + (\lambda_h^{n-1}, \varphi)_{0,h}, \forall (v, \varphi) \in \mathcal{U}_h. \quad (48)$$

Let us introduce p_h^{n-1} as the unique solution in $V_{0,h}$ of the following Dirichlet problem (discrete adjoint problem)

$$\int_{\Omega_h} \nabla p_h^{n-1} \cdot \nabla \theta d\mathbf{x} = (\lambda_h^{n-1}, \theta)_{0,h}, \quad \forall \theta \in V_{0,h}. \quad (49)$$

Consider now $(v, \varphi) \in \mathcal{U}_h$ and take $\theta = \varphi$ in (49); it follows then from (49) and from the definition of \mathcal{U}_h (see Section 6.2) that

$$(\lambda_h^{n-1}, \varphi)_{0,h} = \int_{\Omega_h} \nabla p_h^{n-1} \cdot \nabla \varphi d\mathbf{x} = (p_h^{n-1}, v)_{0,h} \quad (50)$$

Combining (48) and (50), we obtain

$$u_h^n = \frac{1}{r} (X_h^n + p_h^{n-1}). \quad (51)$$

Let us summarize: to obtain (u_h^n, ψ_h^n) solution of problem (44), one may proceed as follows:

- (i) Solve the Dirichlet problem (49) to obtain p_h^{n-1} and, then, use (51) to compute u_h^n ;
- (ii) Obtain $\psi_h^n \in V_{0,h}$ from u_h^n by solving the discrete Dirichlet problem $\int_{\Omega_h} \nabla \psi_h^n \cdot \nabla \theta d\mathbf{x} = (u_h^n, \theta)_{0,h}, \quad \forall \theta \in V_{0,h}.$

6.3.3. On the Solution of Problem (45) Let $Y_h^n = ru_h^n + \ell_h^n$. It follows from (41) that (45) reduces to

$$\min_{z \in \mathcal{S}_{2h}^+} \frac{r}{2} (z, z)_{0,h} - (z, Y_h^n)_{0,h}.$$

Since $z \in \mathcal{S}_{2h}^+$, $(z, z)_{0,h} = 1$, and this problem reduces to

$$\min_{z \in \mathcal{S}_{2h}^+} -(Y_h^n, z)_{0,h} = - \max_{z \in \mathcal{S}_{2h}^+} (Y_h^n, z)_{0,h}.$$

Let us define $(Y_h^n)^+ \in V_{0,h}$ by $(Y_h^n)^+(P_j) = \max(0, Y_h^n(P_j))$, for all $j = 1, \dots, N_{0h}$. If $\max_{j=1, \dots, N_{0h}} Y_h^n(P_j) > 0$, it follows from the Schwarz inequality in $V_{0,h}$ equipped with the $(\cdot, \cdot)_{0,h}$ -scalar product that the solution y_h^n of (45) is given by $y_h^n = (Y_h^n)^+ / \|(Y_h^n)^+\|_{0,h}$. If $(Y_h^n)^+(P_j) = 0$, for all $j = 1, \dots, N_{0h}$, we take for y_h^n an arbitrary element of \mathcal{S}_{2h}^+ (note that the comments at the end of Section 5.4 still apply here).

6.3.4. *On the Solution of Problem (46)* Problem (46) reduces to

$$\min_{\mu \in A_h^+} -(\mu, \psi_h^n)_{0,h} = - \max_{\mu \in A_h^+} (\mu, \psi_h^n)_{0,h}. \quad (52)$$

If $\max_{\mathbf{x} \in \overline{\Omega}_h} \psi_h^n(\mathbf{x}) = 0$, take $\lambda_h^n = 0$; otherwise, if $\max_{\mathbf{x} \in \overline{\Omega}_h} \psi_h^n(\mathbf{x}) > 0$, there exists an index $j_0^n \in \{1, \dots, N_{0h}\}$ such that $\psi_h^n(P_{j_0^n}) = \max_{\mathbf{x} \in \overline{\Omega}_h} \psi_h^n(\mathbf{x})$. Consider now $\lambda_{j_0^n}$ defined by $\lambda_{j_0^n} = (3/A_{j_0^n})w_{j_0^n}$, where $w_{j_0^n} \in V_{0h}$ satisfies $w_{j_0^n}(P_{j_0^n}) = 1$, and $w_{j_0^n}(P_k) = 0$, for all $k = 1, \dots, N_{0h}$, $k \neq j_0^n$. The function $\lambda_{j_0^n}$ is an *approximation of the Dirac measure* at $P_{j_0^n}$; moreover it satisfies

$$\lambda_{j_0^n} \in A_h^+, (\lambda_{j_0^n}, \psi_h^n)_{0,h} = \psi_h^n(P_{j_0^n}) = \max_{\mathbf{x} \in \overline{\Omega}_h} \psi_h^n(\mathbf{x}). \quad (53)$$

From (53), we show that $\lambda_{j_0^n}$ is a solution of the optimization problem (52) if $\max_{\mathbf{x} \in \overline{\Omega}_h} \psi_h^n(\mathbf{x}) \neq 0$, implying that we can take $\lambda_h^n = \lambda_{j_0^n}$ (and complete the search for the solution of (46)).

Remark 4. Suppose that the algorithm (43)–(47) converges; the non-negative function ψ_h produced by the algorithm takes its maximum value at the vertex P_{j_0} . The least we can do is check that, indeed, P_{j_0} maximizes over the set Σ_{j_0} the function $\mathbf{X} \rightarrow (g_{\mathbf{X}}, g_{\mathbf{X}})_{0,h}$, with Σ_{j_0} and $g_{\mathbf{X}} \in V_{0,h}$ are defined respectively by $\Sigma_{j_0} = \{P : P \text{ is a vertex of those triangles of } \mathcal{T}_h \text{ which have } P_{j_0} \text{ as a common vertex}\}$, and $\int_{\Omega_h} \nabla g_{\mathbf{X}} \cdot \nabla \theta d\mathbf{x} = \theta(\mathbf{X})$, for all $\theta \in V_{0,h}$. This would ensure that the solution is (at least) a *local maximum*.

7. Finite Element Implementation of the Green's Function Based Strategy

Using the same notation as in Section 6, we briefly describe the approximation of (20) with piecewise linear finite element approximations. A *steepest descent algorithm* has been discussed in (35) for some particular case.

Following the algorithm using derivatives (derivative-free algorithms will not be discussed here), the approximated algorithm reads as follows. Starting with $\mathbf{X}_0 \in \Omega_h$ given, we iterate for $k \geq 0$:

- (i) Solve the Green's function problem: find $g_h \in V_{0,h}$ satisfying

$$\int_{\Omega_h} \nabla g_h \cdot \nabla v_h d\mathbf{x} = v_h(\mathbf{X}_k), \quad \forall v_h \in V_{0,h}.$$

- (ii) Solve the adjoint problem: find $p_h \in V_{0,h}$ satisfying

$$\int_{\Omega_h} \nabla p_h \cdot \nabla v_h d\mathbf{x} = (g_h, v_h)_{0,h}, \quad \forall v_h \in V_{0,h}.$$

- (iii) Compute the direction \mathbf{D}^k . In order to do so, let us introduce $W_h = \{v \in L^2(\Omega_h) : v|_T \in \mathbb{P}_0, \forall T \in \mathcal{T}_h\}$. By differentiating $p_h \in V_{0,h}$, we obtain $\nabla p_h \in W_h$, a piecewise constant approximation of ∇p . We compute a continuous piecewise linear approximation of ∇p , denoted by $\mathbf{q}_h \in (V_{0,h})^2$, by computing the L^2 -projection of ∇p_h on $(V_{0,h})^2$ with the following relation: find $\mathbf{q}_h \in (V_{0,h})^2$ such that

$$(\mathbf{q}_h, v_h) = (\nabla p_h, v_h)_{0,h}, \quad \forall v_h \in (V_{0,h})^2. \quad (54)$$

We evaluate \mathbf{q}_h at the current iterate and set $\mathbf{D}^k = \mathbf{q}_h(\mathbf{X}^k)$.

- (iv) Compute a *step-length* α_k (many strategies can be found *e.g.* in (10; 33), but are not discussed here).
 (v) Update the iterate:

$$\mathbf{X}_{k+1} = \mathbf{X}_k + \alpha_k \mathbf{D}^k. \quad (55)$$

Numerical results obtained with this approach are given in Section 8.

8. Applications and Numerical Results

We present in this section the results of numerical experiments, obtained by applying to a variety of two-dimensional domains the augmented Lagrangian method discussed in the preceding sections; convergence results are presented when exact solutions are known. Also, for cross-validation purposes, the results obtained via the augmented Lagrangian approach are compared to those obtained using the Green's function based strategy (algorithm (55)).

8.1. Convergence on the Unit Disk

We consider the unit disk $\mathcal{S}_1 = \{\mathbf{x} = (x_1, x_2) : \sqrt{x_1^2 + x_2^2} < 1\}$. When $\Omega = \mathcal{S}_1$, the exact value of the constant γ is given by $\frac{1}{2\sqrt{2\pi}} \simeq 0.19947$, as shown in (13).

In Figure 1, we have visualized the solution ψ_h of problem (39). The value of the augmentation parameter is $r = 10^{-2}$ (which corresponds to *large* time steps for an *alternating direction implicit* (ADI)

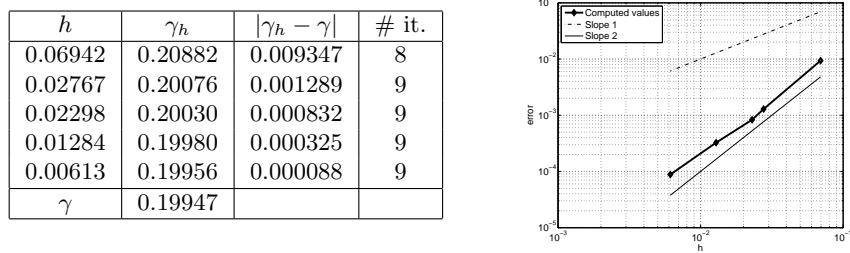


Fig. 2. Augmented Lagrangian based strategy: left: values of γ_h for the unit disk and number of iterations of the augmented Lagrangian algorithm; right: convergence (log-log scale) of the error $|\gamma_h - \gamma|$ for the unit disk.

suggested, the optimal Green function is indeed $\mathbf{y} \rightarrow G(\mathbf{C}, \mathbf{y})$, with $\mathbf{C} = (1/2, 1/2)$.

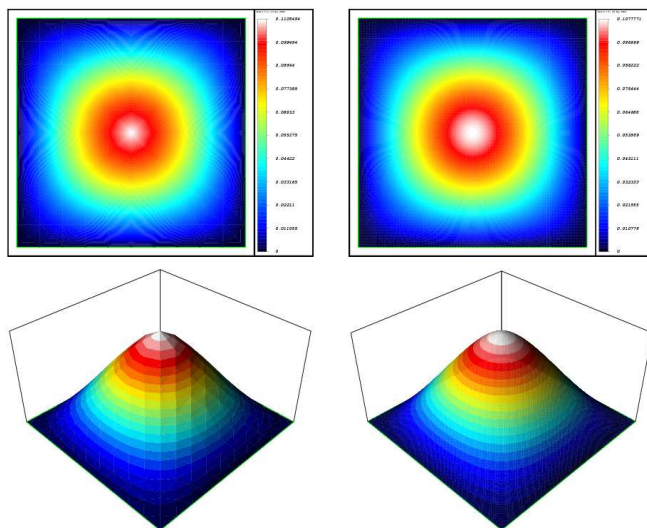


Fig. 3. Augmented Lagrangian based strategy: Solution ψ_h corresponding to the approximation γ_h of the constant γ for the unit square Ω_S for $h = 1/10$ (left) and $1/80$ (right).

Figure 4 visualizes the solution ψ_h on Ω_T for various mesh sizes h , while Table 2 illustrates the values taken by γ_h , as well as the location of the maximum of the solution ψ_h , and the number of iterations of the Uzawa algorithm.

Numerical results are consistently showing around 8–10 iterations for the augmented Lagrangian algorithm. The maximizer of ψ_h is lo-

Table 1. Augmented Lagrangian based strategy: Values of the approximation γ_h for Ω_S , number of iterations of the augmented Lagrangian algorithm, and location of the ψ_h maximizer.

h	γ_h	Location	# it.
0.05000	0.110549	(0.5, 0.5)	8
0.02500	0.108557	(0.5, 0.5)	8
0.01250	0.107953	(0.5, 0.5)	8
0.00625	0.107777	(0.5, 0.5)	8

cated near the center of the inscribed circle inside Ω_T , with the largest inradius (but not exactly equal to it). This location is accurate and consistent up to the mesh size, but depends on the local properties of the mesh. This remark is consistent with theoretical investigations presented for instance in (1), where the largest inradius is identified as the main criterion for the determination of the eigenvalues of the Laplacian operator.

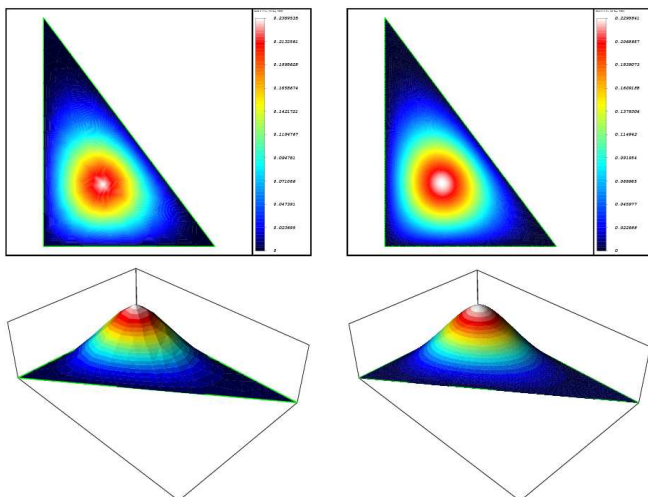


Fig. 4. Augmented Lagrangian based strategy: Solution ψ_h corresponding to the approximation γ_h of the constant γ for Ω_T for $h = 0.13308$ (left) and 0.01159 (right).

8.3. Validation with the Green's Functions Based Strategy

The numerical results obtained with the augmented Lagrangian based method can be validated by comparing with the results obtained

Table 2. Augmented Lagrangian based strategy: Values of the approximation γ_h for Ω_T , number of iterations of the iterative algorithm, and location of the ψ_h maximizer.

h	γ_h	Location	# it.
0.13308	0.236953	(1.04103, 1.08259)	9
0.05793	0.234287	(0.97132, 1.07262)	9
0.02909	0.230355	(1.01081, 1.11609)	9
0.01159	0.229884	(1.00024, 1.11437)	9

using the Green's function based method. First, Figure 5 visualizes the contours of the function $\mathbf{X} \rightarrow \|G(\mathbf{X}, \cdot)\|_{L^2(\Omega)}$. The best constant γ given by (20) is the maximum of the function under consideration.

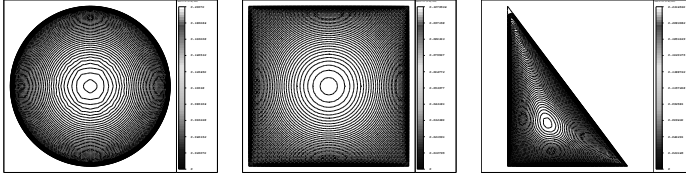


Fig. 5. Contours of the function $\mathbf{X} \rightarrow \|G(\mathbf{X}, \cdot)\|_{L^2(\Omega)}$. Left: disk domain; middle: square domain; right: triangular domain.

One sees that the solution obtained with the augmented Lagrangian algorithm is the optimal one, in the sense that the point $\bar{\mathbf{X}}$ that maximizes the function ψ in Figures 1, 3 and 4, is also the maximizer of the function $\mathbf{X} \rightarrow \|G(\mathbf{X}, \cdot)\|_{L^2(\Omega)}$ as seen in Figure 5 (left, middle and right resp.). Figure 6 shows the solution obtained with the algorithm (55) for the unit disk (left, starting from $\mathbf{X}^0 = (-0.7, 0.7)$), for the triangular domain (middle, with $\mathbf{X}^0 = (0.11, 3.63)$), and for the unit square (right, with $\mathbf{X}^0 = (0.05, 0.05)$). The iterative algorithm provides a solution satisfying $\|\mathbf{X}^k - \mathbf{X}^{k-1}\|_2 \leq 10^{-5}$ in approx. 50–100 iterations, with $\alpha_k = 1.0$. For these three cases, algorithm (55) generates iterates along a straight line going from the initial guess to the exact solution. Table 3 shows a comparison between the values of $\bar{\mathbf{X}}$ obtained with both algorithms.

These results validate the augmented Lagrangian based methodology, and show that it is actually much more efficient (around 10 iterations vs. around 50, each method requiring the solution of two discrete Poisson problems at each iteration), without sacrificing the accuracy of the solution.

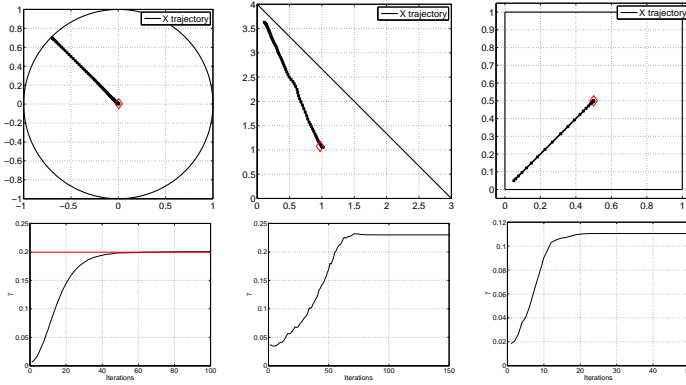


Fig. 6. Convergence of the Green's function based algorithm for the unit disk (left $h = 0.02298$), triangular (middle, $h = 0.05793$), and unit square domains (right, $h = 0.05$). Top row: trajectory of the iterates \mathbf{X}^k obtained with the descent algorithm (55), and location of the maximizer obtained with the augmented Lagrangian method; Bottom row: evolution of the values of $\gamma^k := \|G(\mathbf{X}^k, \cdot)\|_{L^2(\Omega)}$.

Table 3. Comparison of the augmented Lagrangian and Green's function based methods.

		Location	γ	# it.
Circle ($h = 0.02298$)	Aug. Lag.	(0.0040000, 0.0040000)	0.20030	9
	Green's	(0.00356945, 0.00407292)	0.20027782	100
Triangle ($h = 0.05793$)	Aug. Lag.	(0.97132, 1.07262)	0.234287	9
	Green's	(1.01483350, 1.05234727)	0.22986620	130
Square ($h = 0.05$)	Aug. Lag.	(0.5, 0.5)	0.110549	8
	Green's	(0.5, 0.5)	0.11054942	50

8.4. Non-Convex and Non Simply Connected Domains

The presented framework is theoretically valid when the considered domain Ω is either convex or non-convex but with a smooth boundary Γ . In this subsection, we show that the augmented Lagrangian based methodology is also efficient for non-convex domains, even when those may have a non-smooth boundary (in the case, for instance, of re-entrant corners). To do so, let us consider first the *ring-shaped* domain $\mathcal{S}_{\frac{1}{2}1} = \left\{ (x_1, x_2) \in \mathbb{R}^2 : \frac{1}{2} < \sqrt{x_1^2 + x_2^2} < 1 \right\}$.

Figure 7 visualizes the solution ψ_h for Ω_S for two different mesh sizes h , while Table 4 illustrates the values taken by γ_h , as well as the maximizer of ψ_h , and the number of iterations of the Uzawa algorithm. Observe that this problem being a highly degenerated generalized eigenvalue problem, the proposed algorithm selects a particular

eigenfunction, but the solution can be rotated without changing the value of the objective function, depending on the initial guess and the mesh.

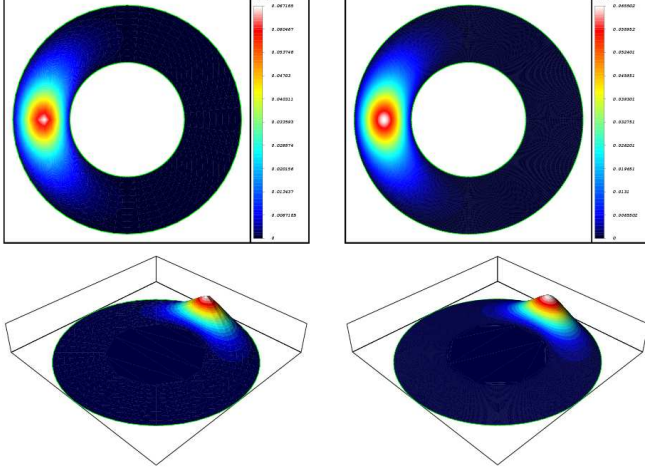


Fig. 7. Augmented Lagrangian based strategy: Solution ψ_h corresponding to the approximation γ_h of the constant γ for the ring-shaped domain $\mathcal{S}_{\frac{1}{2},1}$ for $h = 0.04062$ (left) and 0.00614 (right).

Table 4. Augmented Lagrangian based strategy: Values of the approximation γ_h for $\mathcal{S}_{\frac{1}{2},1}$, number of iterations of the augmented Lagrangian algorithm, and location of the maximizer of the function ψ_h .

h	γ_h	Location	# it.
0.04062	0.067185	(-0.71822, 0.00400)	9
0.01914	0.066029	(-0.74084, 0.00400)	9
0.00930	0.065527	(-0.72677, 0.00400)	9
0.00614	0.065502	(-0.73329, 0.00400)	9

Figure 8 (left) visualizes in the ring domain the contours of the function $\mathbf{X} \rightarrow \|G(\mathbf{X}, \cdot)\|_{L^2(\Omega)}$, emphasizing the radial invariance of the function, and the degeneracy of the eigenvalue problem. The best constant γ given by (20) is the maximum of the illustrated function. Figure 8 (right) shows the profile of $\|G(\mathbf{X}, \cdot)\|_{L^2(\Omega)}$ along a cut in the radial direction; the solution obtained with the augmented Lagrangian approach, whose location is illustrated by the vertical line, satisfies the given maximum up to the mesh resolution.

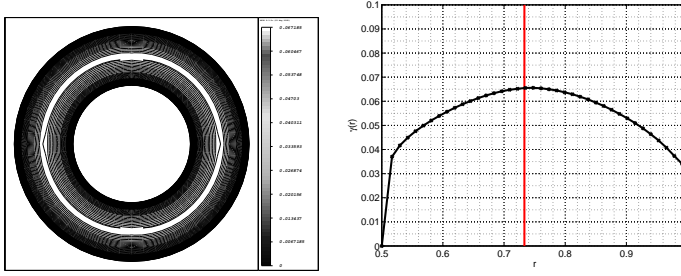


Fig. 8. Green's function based strategy: Left: contours of the function $\mathbf{X} \rightarrow \|G(\mathbf{X}, \cdot)\|_{L^2(\Omega)}$. Right: cut along a radial direction, and comparison with the solution obtained with the augmented Lagrangian approach (located at the vertical line).

Finally, let us discuss the behavior of γ_h as a function of the angle of a re-entrant corner. In order to do so, consider the "pie-shaped" domain Ω_θ defined by

$$\Omega_\theta = \left\{ (x_1, x_2) \in \mathbb{R}^2 : \begin{pmatrix} x_1 \\ x_2 \end{pmatrix} = \begin{pmatrix} r \cos \phi \\ r \sin \phi \end{pmatrix}, 0 < r < 1, \theta < \phi < 2\pi - \theta \right\}.$$
 Let us also define $\omega = 2\pi - 2\theta$ (the angle inside the domain Ω_θ). The notation is illustrated on Figure 9.

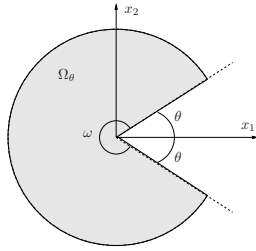


Fig. 9. Pie-shaped domain Ω_θ . Sketch and notation.

When $\theta \rightarrow 0$, the domain tends to the unit disk *with a slit*, that is well-known to produce strong singularities at the extremity of the slit (23; 24). Figure 10 visualizes the solution ψ_h associated with Ω_θ and $h \simeq 0.01$ for various values of θ , ranging from 0 to $\pi/4$. Observe that the symmetry is preserved.

Table 5 illustrates the values taken by γ_h , as well as the location of the optimal function ψ_h for various values of θ , and the number of iterations of the Uzawa algorithm. One observes that the value of γ_h increases linearly when $\theta \rightarrow 0$.

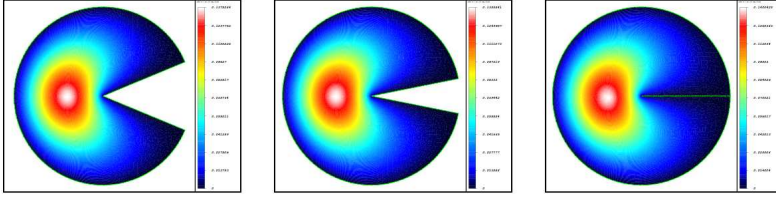


Fig. 10. Augmented Lagrangian based strategy: Solution ψ_h corresponding to the approximation γ_h for Ω_θ , for $\omega = 7\pi/4, 15\pi/8$ and 2π respectively (left to right).

Table 5. Augmented Lagrangian based strategy: Values of the approximation γ_h for Ω_θ , number of iterations of the augmented Lagrangian algorithm, and location of the maximizer of the function ψ_h .

ω	h	γ_h	Location	# it.
2π	0.010197	0.140042	(-0.36858, -0.01751)	17
$23\pi/12$	0.010083	0.139609	(-0.38865, 0.02002)	17
$15\pi/8$	0.010193	0.138884	(-0.38847, -0.00217)	17
$7\pi/4$	0.010119	0.137528	(-0.39293, -0.00433)	17
$3\pi/2$	0.009711	0.134045	(-0.41354, 0.01683)	17

Finally, numerical results obtained with the Green's function based strategy are presented for the domain with a slit. Figure 11 (left) visualizes the contours of the function $\mathbf{X} \rightarrow \|G(\mathbf{X}, \cdot)\|_{L^2(\Omega)}$. The best constant γ given by (20) is the maximum of the illustrated function. Note that the function is *quite flat* around its maximum.

Figure 11 (middle) shows the trajectory obtained with the algorithm (55), starting from $\mathbf{X}^0 = (0.95, 0.05)$. The above algorithm provides a solution satisfying $\|\mathbf{X}^k - \mathbf{X}^{k-1}\|_2 \leq 10^{-2}$ in approximately 1000 iterations, with $\alpha_k = 10.0$, and encounters difficulties in converging to the exact solution. Figure 11 (right) visualizes the approximation of γ obtained at each iterate. The flat profile of the objective function creates convergence problems, and the better convergence properties of the augmented Lagrangian method are obvious here. Solutions comparisons are given in Table 6.

Table 6. Comparisons between the augmented Lagrangian and Green's function based strategies.

Slit domain		Location	γ	# it.
$(h = 0.010197)$	Aug. Lag.	(-0.36858, -0.01751)	0.140042	17
	Green's	(-0.40034, 0.09696)	0.139641	100

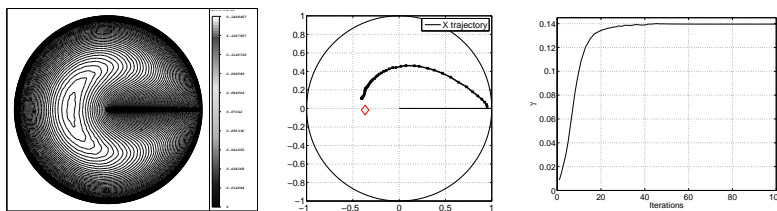


Fig. 11. Green's function based strategy for the domain with a slit: Left: contours of the function $\mathbf{X} \rightarrow \|G(\mathbf{X}, \cdot)\|_{L^2(\Omega)}$; middle: trajectory of the iterates \mathbf{X}^k ; right: evolution of the values of $\gamma^k := \|G(\mathbf{X}^k, \cdot)\|_{L^2(\Omega)}$.

Acknowledgements. The authors acknowledge the partial support of the National Science Foundation (Grant NSF-DMS 0913982). The first author gratefully acknowledges the support of MATHICSE, EPFL, for funding his sabbatical leave (2009-2010).

References

1. R. Bañuelos. Sharp estimates for Dirichlet eigenfunctions in simply connected domains. *J. Diff. Eq.*, 125:282–298, 1996.
2. R. Brent. *Algorithms for Minimization Without Derivatives*. Prentice Hall, Englewood Cliffs, NJ, 1973.
3. A. Caboussat and R. Glowinski. Numerical methods for the vector-valued solutions of non-smooth eigenvalue problems. *J. Sci. Comp.*, submitted, 2009.
4. A. Caboussat and R. Glowinski. Numerical solution of a non-smooth variational problem arising in stress analysis : The scalar case. *Int. J Numer. Anal. Model.*, 6(3):402–419, 2009.
5. A. Caboussat and R. Glowinski. Numerical solution of a non-smooth variational problem arising in stress analysis : The vector case. *Discrete Contin. Dyn. Syst. A*, 27(4):1447–1472, 2010.
6. A. Caboussat, R. Glowinski, and V. Pons. An augmented Lagrangian approach to the numerical solution of a non-smooth eigenvalue problem. *J. Numer. Math*, 17(1):3–26, 2009.
7. T. Chan and J. Shen. *Image Processing and Analysis: Variational, PDE, Wavelet, and Stochastic Methods*. SIAM, Philadelphia, 2005.
8. P. G. Ciarlet. Basic error estimates for elliptic problems. In P.G. Ciarlet and J.L. Lions, editors, *Handbook of Numerical Analysis*, volume II, pages 17–351. North-Holland, Amsterdam, 1991.
9. F. H. Clarke. *Optimization and Nonsmooth Analysis*, volume 5 of *Classics in Applied Mathematics*. SIAM, Philadelphia, 1990.

10. A. R. Conn, K. Scheinberg, and L. N. Vicente. *Introduction to Derivative-Free Optimization*. MPS-SIAM Series on Optimization. SIAM, Philadelphia, PA, 2009.
11. R. Courant and D. Hilbert. *Methods of Mathematical Physics*. Wiley Interscience, New York, NY, 1989.
12. E. J. Dean and R. Glowinski. Numerical solution of the two-dimensional elliptic Monge-Ampère equation with Dirichlet boundary conditions: an augmented Lagrangian approach. *C. R. Acad. Sci. Paris, Sér. I*, 336:779–784, 2003.
13. E. J. Dean and R. Glowinski. An augmented Lagrangian approach to the numerical solution of the Dirichlet problem for the elliptic Monge-Ampère equation in two dimensions. *Electronic Transactions in Numerical Analysis*, 22:71–96, 2006.
14. E. J. Dean and R. Glowinski. Numerical methods for fully nonlinear elliptic equations of the Monge-Ampère type. *Comp. Meth. Appl. Mech. Engrg.*, 195:1344–1386, 2006.
15. M. Degiovanni and V. Radulescu. Perturbations of nonsmooth symmetric nonlinear eigenvalue problems. *C. R. Acad. Sci., Paris*, 329:281–286, 1999.
16. I. Ekeland and R. Temam. *Convex Analysis and Variational Problems*. North-Holland, Amsterdam, New York, 1976.
17. L. C. Evans. *Partial Differential Equations*. American Mathematical Society, third edition, 2002.
18. M. Fortin and R. Glowinski. *Augmented Lagrangian Methods: Applications to the Numerical Solution of Boundary-Value Problems*. Studies in Mathematics and Its Applications. Elsevier Science Ltd, 1983.
19. R. Glowinski, T. Kärkäinen, T. Valkonen, and A. Ivannikov. Nonsmooth SOR for L^1 -fitting: Convergence study and discussion of related issues. *J. Sci. Comp.*, 37:103–138, 2008.
20. R. Glowinski, J.-L. Lions, and J. W. He. *Exact and Approximate Controllability for Distributed Parameter Systems: A Numerical Approach*. Encyclopedia of Mathematics and its Applications. Cambridge University Press, 2008.
21. R. Glowinski, J.-L. Lions, and R. Trémoières. *Numerical Analysis of Variational Inequalities*. North Holland, 1981.
22. R. Glowinski and P. Le Tallec. *Augmented Lagrangians and Operator-Splitting Methods in Nonlinear Mechanics*. SIAM, Philadelphia, 1989.
23. P. Grisvard. *Elliptic Problems in Nonsmooth Domains*. Pitman Advanced Publ. Program, 1985.

24. P. Grisvard. *Singularities in Boundary Value Problems*. Masson, 1992.
25. M. Hegland and J. T. Marti. Numerical computation of least constants for the Sobolev inequality. *Numer. Math.*, 48:607–616, 1986.
26. B. Kawohl and F. Schuricht. Dirichlet problems for the 1-Laplace operator including the eigenvalue problem. *Communications in Contemporary Mathematics*, 9(4):515–543, 2007.
27. V. K. Le, D. Motreanu, and V. V. Motreanu. On a non-smooth eigenvalue problem in Orlicz-Sobolev spaces. *Applicable Analysis*, 89:229–242, 2010.
28. E. H. Lieb. Sharp constants in the Hardy-Littlewood-Sobolev and related inequalities. *Ann. of Math. (2)*, 118(2):349–374, 1983.
29. J.-L. Lions. *Optimal control of systems governed by partial differential equations*. Springer-Verlag, berlin, New York, 1971.
30. K. Majava, R. Glowinski, and T. Kärkkäinen. Solving a non-smooth eigenvalue problem using operator-splitting methods. *Int. J. Comput. Math.*, 84(6):825–846, 2007.
31. J. T. Marti. Evaluation of the least constant in Sobolev’s inequality for $H^1(0, s)$. *SIAM J. Numer. Anal.*, 20(6):1239–1242, 1983.
32. J. Nečas. *Introduction to the Theory of Nonlinear Elliptic Equations*. John Wiley & Sons, 1986.
33. J. Nocedal and S. J. Wright. *Numerical optimization*. Springer Series in Operations Research and Financial Engineering. Springer, New York, second edition, 2006.
34. M. J. D. Powell. An efficient method for finding the minimum of a function of several variables without calculating derivatives. *Computer Journal*, 7:152–162, 1964.
35. W. Richardson. Steepest descent and the least C for Sobolev’s inequality. *Bull. London Math. Soc.*, 18(5):478–484, 1986.
36. H. C. Rodrigues, J. M. Guedes, and M. P. Bendsoe. Necessary conditions for optimal design of structures with a non-smooth eigenvalue based criterion. *Structural Optimization*, 9:52–56, 1995.
37. G. Rosen. Minimum value for c in the Sobolev inequality $\|\phi^3\| \leq c\|\nabla\phi\|^3$. *SIAM J. Appl. Math.*, 21:30–32, 1971.
38. G. Talenti. Best constant in Sobolev inequality. *Ann. Mat. Pura Appl. (4)*, 110:353–372, 1976.
39. K. Watanabe, Y. Kametaka, A. Nagai, K. Takemura, and H. Yamagishi. The best constant of Sobolev inequality on a bounded interval. *J. Math. Anal. Appl.*, 340:699–706, 2008.